

PROCEEDINGS OF SPIE

[SPIDigitalLibrary.org/conference-proceedings-of-spie](https://spiedigitallibrary.org/conference-proceedings-of-spie)

An optofluidic channel model for in vivo nanosensor networks in human blood

Pedram Johari, Josep M. Jornet

Pedram Johari, Josep M. Jornet, "An optofluidic channel model for in vivo nanosensor networks in human blood," Proc. SPIE 10206, Disruptive Technologies in Sensors and Sensor Systems, 1020607 (2 May 2017); doi: 10.1117/12.2262824

SPIE.

Event: SPIE Defense + Security, 2017, Anaheim, California, United States

An Optofluidic Channel Model for In Vivo Nanosensor Networks in Human Blood

Pedram Johari and Josep M. Jornet

Department of Electrical Engineering
University at Buffalo, The State University of New York
Buffalo, NY 14260, USA

ABSTRACT

In vivo Wireless Nanosensor Networks (iWNSNs) consist of nano-sized communicating devices with unprecedented sensing and actuation capabilities, which are able to operate inside the human body. iWNSNs are a disruptive technology that enables the monitoring and control of biological processes at the cellular and sub-cellular levels. Compared to *ex vivo* measurements, which are conducted on samples extracted from the human body, iWNSNs can track (sub) cellular processes when and where they occur. Major progress in the field of nanoelectronics, nanophotonics and wireless communication is enabling the interconnection of nanosensors. Among others, plasmonic nanolasers with sub-micrometric footprint, plasmonic nano-antennas able to confine light in nanometric structures, and single-photon detectors with unrivaled sensitivity, enable the communication among implanted nanosensors in the near infrared and optical transmission windows. Motivated by these results, in this paper, an optofluidic channel model is developed to investigate the communication properties and temporal dynamics between a pair of *in vivo* nanosensors in the human blood. The developed model builds upon the authors' recent work on light propagation modeling through multi-layered single cells and cell assemblies and takes into account the geometric, electromagnetic and microfluidic properties of red blood cells in the human circulatory system. The proposed model guides the development of practical communication strategies among nanosensors, and paves the way through new nano-biosensing strategies able to identify diseases by detecting the slight changes in the channel impulse response, caused by either the change in shape of the blood cells or the presence of pathogens.

Keywords: *In vivo* Wireless Nanosensor Networks; Optofluidic Channel Model; Wireless Communications; Nano-biosensing; Temporal Dynamics of In Vivo Nanosensors.

1. INTRODUCTION

Major progress in the field of bio-photonics is enabling the control and monitoring of biological processes through the utilization of light. For instance, by incorporating light-actuated/light-emitting proteins into cells, key biological processes can be controlled and monitored in real time.^{1,2} One of the interesting characteristics of the optical signals is their very small wavelength, which theoretically enables precise temporal and spatial control and monitoring. Currently, most of the existing studies rely only on traditional optical sources and detectors, which, due to their size and capabilities, limit the applications of light-mediated bio-interfaces. Nanotechnology is providing the engineering community with a new set of tools to create novel nanoscale devices with unprecedented functionalities. These include, among others, plasmonic nano-lasers with sub-micrometric footprint,³ plasmonic nano-antennas able to confine light in nanometric structures,⁴ or single-photon detectors with unrivaled sensitivity.⁵ Plasmonic nano-lasers working in conjunction with nano-antennas can serve as nano-actuators of light-controlled processes. Similarly, nano-detectors enhanced with plasmonic nano-antennas can act as nanosensors. As a result of all these improvements, it is not beyond imagination that within a few years we will see these emerging nanomachines in our daily life with remarkable applications ranging from healthcare monitoring wearable devices and intra-body microfluidic nanomachines to brain-machine interface implants.⁶

Further author information: (Send correspondence to Pedram Johari)

Pedram Johari: E-mail: pedramjo@buffalo.edu, Telephone: 1 (716) 907-3086

Josep M. Jornet: E-mail: jmjornet@buffalo.edu, Telephone: 1 (716) 645-1607

Disruptive Technologies in Sensors and Sensor Systems, edited by Russell D. Hall, Misty Blowers, Jonathan Williams,
Proc. of SPIE Vol. 10206, 1020607 · © 2017 SPIE · CCC code: 0277-786X/17/\$18 · doi: 10.1117/12.2262824

By means of communications, these nanomachines will be able to autonomously communicate among themselves or with a control/monitoring center to transmit their sensing information, receive the controlling commands, and coordinate joint actions when needed. The resulting iWNSNs enable smart health-monitoring and drug-delivery systems, among many others. Within several recently proposed wireless technologies that could enable the communication between nanomachines, the molecular and electromagnetic communications are the leading ones. The molecular communication path has been thoroughly investigated.^{7,8} This mechanism is naturally used by biological cells to exchange information and could be enabled by means of synthetic biology; however, the very low achievable data rates severely limit the efficiency of nanosensor networks.⁹ From the electromagnetic perspective, emerging plasmonic nanoantennas have been recently enabled the wireless communication among nano-devices at very high frequencies, ranging from the Terahertz (THz) band (0.10-10 THz)¹⁰ to the infra-red and visible optical range.⁴ The propagation of THz-band waves inside the human body is drastically impacted by the absorption of liquid water molecules and causes internal vibrations into molecules, which results in heat and could lead to photothermal tissue damage. Alternatively, the majority of existing nano-bio-sensing technologies rely on the use of light due to the fact that the molecular absorption of liquid water is minimal in the optical window (between 400 THz and 750 THz).¹¹

In this direction and in order to analyze the feasibility of intra-body wireless optical communications, one of the most important challenges is to understand the propagation properties of light in biological scenarios. Traditional channel models for light propagation in biological tissues¹²⁻¹⁴ cannot accurately describe the channel properties in nanoscale scenarios because of several reasons. First of all, in intra-body NanoScale Optical (NSO) communications the wavelength range of study is in the order of several hundreds of nanometers; therefore, due to the relatively large particles -compared to the wavelength-, and short range communication distances, the macroscopic properties of different particles cannot describe the details of propagation pattern of the light in nanoscale. Furthermore, the radiated light from a nano-antenna covers a much smaller area than that of the external macroscopic laser; hence, the wave does not radiate through a large enough number of cells to be dealt with as an isotropic medium. In view of the aforementioned drawbacks, we have studied the propagation pattern of the light in human blood by analyzing the impact of single cells rather than a homogeneous material, and have developed a detailed channel model for intra-body NSO communications.^{15,16} However, the temporal and spatial dynamics of the cells and possibly the floating nanomachines play a significant role in the transmission and detection of the intra-body NSO communication systems and has not been investigated in the literature to this point.

In this paper, we develop an optofluidic channel model to investigate the communication properties and temporal dynamics between a pair of *in vivo* nanosensors in the human blood. In particular, we start with a system model for the human circulatory system, in which we consider a blood vessel containing moving blood cells along with nanomachines. Then we develop a novel complete communication model which we build upon our recent works^{15,16} on light propagation modeling through multi-layered single cells and cell assemblies by taking into account the geometric, electromagnetic and microfluidic properties of Red Blood Cells (RBCs) in the human circulatory system. Thanks to the light focusing property of the RBCs and by utilizing simple and feasible modulation/demodulation schemes and transmission/detection methods, we show that optical wireless communication is a promising technique for future iWNSNs. In fact, recently it has been experimentally¹⁷ and theoretically¹⁶ shown that RBCs perform as optofluidic micro-lenses inside the human blood. This eases the propagation of the light inside the human blood by reducing the exponential path loss due to the scattering and focusing the light in narrower beams through longer distances. The proposed model conducts the development of practical communication strategies among autonomous in-vivo nano-bio-sensors which can operate inside the human body in real time. It also enables new nano-biosensing strategies as a way to provide faster, low-cost, and more accurate disease diagnosis and treatment than traditional technologies. As an specific example, disease identification can be done by detecting the slight changes in the channel impulse response, caused by (sub) cellular abnormalities which may appear in terms of either the change in shape of the blood cells or the presence of pathogens.

The remainder of the paper is organized as follows. In Section 2, we define a system model for optical communication of the nanomachines inside the human blood vessel by considering the dynamics of the human circulatory system. Section 3 contains a dynamic channel model besides the analysis of signal transmission/reception for

iWNSNs. In Section 4, we demonstrate the numerical and multiphysics simulation results, and show the performance of iWNSNs inside the human blood. Finally, we conclude the paper in Section 5.

2. SYSTEM MODEL

In this section, we first provide a human blood vessel model as well as a single cell layered structure model for intra-body communications. Then, a brief overview on the dynamics of the cells inside the human blood is presented.

2.1 Blood Vessel and Layered Cell Model

The propagation of the light is affected in different ways by different types of cells. In this work, we consider the optical communication of nanomachines inside a blood vessel. Human blood is composed by erythrocytes (also known as RBCs), leukocytes (also known as white blood cells), and thrombocytes or Platelets. Among all these, RBCs are the largest (7 microns) and most abundant (45%) and, thus, govern the propagation of light in blood. Furthermore, all the blood cells are floating inside the blood plasma (55% of blood) which is essentially (92%) water.

Therefore, in our scenario, we consider a pair of nanomachines communicating in a blood vessel which contains RBCs floating in plasma (Figure 1 a). Plasma is modeled as a lossy medium with macroscopic properties (complex relative permittivity ϵ_r) of water which mainly captures the effect of the medium on the optical propagating wave. We also consider communicating nanomachines inside the blood. These machines are individual nanomotes which are capable to send/receive and sense/actuate, and can be built by integrating several of the nanomaterial-based nano-components such as nanosensors, nanoactuator, nano-transceiver, nano-memory, nano-antenna, nano-processor, and nano-power generators. The nanomachines are capable to communicate among each other as well as to the outside world (e.g., through on-body mounted wearable devices) by utilizing the spreading of the light in their environment.

Similar to our recent work,¹⁶ each RBC is modeled as a multi-layered sphere each with different complex permittivities (Figure 1 b). The outer shell is the cell membrane (effectively fat), filled with the cytoplasm and the nucleus (which is mainly hemoglobin for RBC). The spherical cell is widely used in simulation and analytical researches.¹²⁻¹⁴ However, the shape of different cells is not necessarily spherical, and the nucleus is not always at the center of it. Nonetheless, the sphere is a general model that is used as a good approximation for all types of cells with different shapes due to the random positions and movement of the cells in different layers of biological tissues. Although the real RBC has a biconcave shape (Figure 1 a), we consider the simplified spherical cell model (Figure 1 b) to provide tractable simulations. We have shown in our recent works^{15,16} that using the spherical model gives an accurate enough approximation of the real RBCs for wireless optical channel modeling.

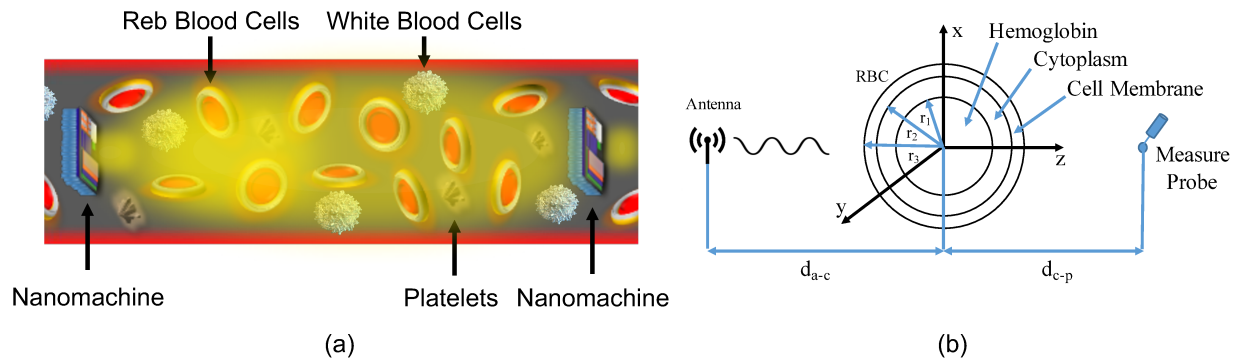


Figure 1. (a) Communication of nanomachines inside the human blood; (b) Layered RBC Model.

2.2 Temporal and Spatial Cell Movements Model

The dynamics of blood flow are referred to as hemodynamics, and the circulatory system is controlled by homeostatic mechanisms. Hemodynamic response continuously monitors and adjusts to conditions in the body and its environment. Thus hemodynamics explains the physical laws that govern the flow of blood in the blood vessels. Blood flow ensures the transportation of nutrients, hormones, metabolic wastes, O_2 and CO_2 throughout the body to maintain cell-level metabolism, the regulation of the pH, osmotic pressure and temperature of the whole body, and the protection from microbial and mechanical harms.¹⁸

Blood is a non-Newtonian fluid (a fluid that does not follow Newton's Law of Viscosity), best studied using rheology rather than hydrodynamics. Blood vessels are not rigid tubes, so classic hydrodynamics and fluids mechanics based on the use of classical viscometers are not capable of explaining hemodynamics.¹⁹ The presence of the formed elements (platelets, white blood cells and red blood cells) in blood and their interaction with plasma molecules are the main reasons why blood differs from ideal Newtonian fluids.¹⁸ Typical values for the viscosity of normal human plasma at 37°C is $1.4\text{ mN}\cdot\text{s}/\text{m}^2$.²⁰ The viscosity of normal plasma varies with temperature in the same way as does that of its solvent water; a 5°C increase of temperature in the physiological range reduces plasma viscosity by about 10%.

In our scenario, we consider that the nanomachines are moving with the same average speed as the RBCs and are designed in a way that they always tend to face through the direction of the blood flow. Without loss of generality, for our model development we further consider that the nanomachines are always fixed (not moving) relative to each other, and only the cells in between have a relative movement. Cells are considered to be moving following the Brownian motion phenomenon, which is the most common model for the particle motion in a fluid. These random movements contain a random direction and a random speed for each of the cells (Figure 2). In mathematics, Brownian motion is described by the Wiener process; a continuous-time stochastic process with stationary independent increments. The Wiener process W_t is characterized by four facts:

1. $W_0 = 0$;
2. W_t is almost surely (with probability one) continuous;
3. W_t has independent increments;
4. $W_t - W_s \sim \mathcal{N}(0, t - s)$ for $0 \leq s \leq t$.

$\mathcal{N}(\mu, \sigma^2)$ denotes the normal distribution with expected value μ and variance σ^2 . The condition that it has independent increments means that if $0 \leq s_1 < t_1 \leq s_2 < t_2$ then $W_{t_1} - W_{s_1}$ and $W_{t_2} - W_{s_2}$ are independent random variables. The unconditional probability density function of the Wiener process W_t is given by:

$$f_{W_t}(x) = \frac{1}{\sqrt{2\pi t}} e^{-x^2/(2t)}. \quad (1)$$

which follows normal distribution with mean $E[W_t] = 0$, and variance $Var(W_t) = t$.

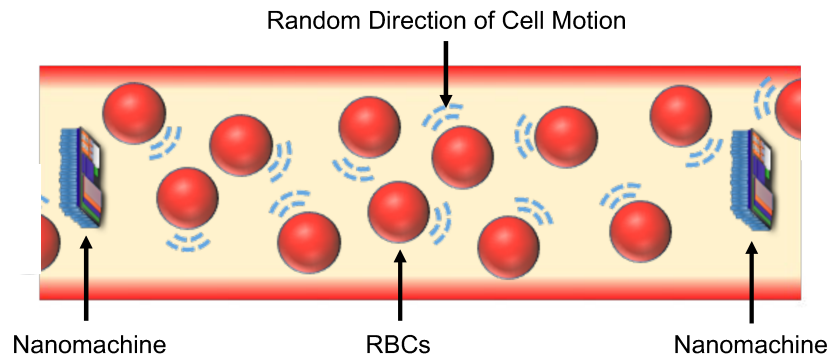


Figure 2. Random movements of the RBCs in between two floating nanomachines.

3. CHANNEL MODEL AND COMMUNICATION ANALYSIS

3.1 Channel Model

Despite scattering, recent studies¹⁵⁻¹⁷ have shown that the RBCs work as the optofluidic lenses and focus the light at a central area after the cell. It can be shown that the intensity of the wave will be increased over the focal line after the cell. This focal line extends over the central line of the cell within the range $r \cdot f(\alpha)$.¹⁶ $f(\alpha)$ can be calculated as follows:

$$f(\alpha) = \frac{\alpha}{\sin \left[2 \left(\arcsin(\alpha) - \arcsin\left(\frac{n_{r,1}}{n_{r,2}}\alpha\right) \right) \right]}, \quad (2)$$

where α is the ratio of d_r to r , where d_r is the distance between the incident optical ray and the central axis of the sphere, and r is the radius of the sphere. $n_{r,1}$ and $n_{r,2}$ are the real part of the refractive index of the medium and the cell respectively. For a wave that is polarized along the x axis and the direction of the propagation is along z axis, it can be shown that the aggregated field coming from the secondary (focusing) rays with parameter α is given by:¹⁶

$$\vec{E}_F^{fr}(\alpha) = \pi \left| \vec{E}_0 \right| \left(\mathcal{L}^{fr,p} \cos(\psi) + \mathcal{L}^{fr,s} \right) \hat{a}_x. \quad (3)$$

Here \vec{E}_0 is the incoming ray coming from the antenna, \hat{a}_x is the unit vector in the direction of x axis, and $\mathcal{L}^{fr,p}$ and $\mathcal{L}^{fr,s}$ represent the total path loss (including the absorption, scattering, and the boundary losses), that every p - and s -polarized secondary (focusing) ray faces in its path to the focal point. Following the same approach the received field coming through the main ray over the focal line (central line of the cell) can be also given as:¹⁶

$$\vec{E}_F^{mr} = \left| \vec{E}_0 \right| \mathcal{L}^{mr} \hat{a}_x, \quad (4)$$

where \mathcal{L}^{mr} is the path loss that the main ray faces in its path to a point on the focal line. Note that \vec{E}_0 is initially considered to be polarized along the x axis and hence propagating through z direction. From equations (3) and (4), it can be seen that the polarization of the received field on the focal line is also along the x axis, and hence propagating through z . This interesting phenomenon only happens when the focusing rays aggregate at a focal point, which causes the intensity of the field to be amplified over the focal line. By utilizing the electric field intensity equations (3) and (4), the channel impulse response on the focal line can be written as:¹⁶

$$H(f, d) = \gamma(r) \cdot \left(\left| \vec{E}_F^{mr} \right| e^{-j\omega\tau_{mr}} + \left| \vec{E}_F^{fr} \right| e^{-j\omega\tau_{fr}} \right), \quad (5)$$

where ω is the angular frequency of the electromagnetic wave, and τ_{mr} and τ_{fr} are the delays that the main and the secondary (focusing) rays experience in their path to the focal point, respectively. $\gamma(r)$ is the cell-size gain factor which is a function of the radius of the cell. The larger the cell, the bigger the surface of the cell that is being exposed to the incoming light, and hence the more energy will be focused at the focal line. In (5), d is the total distance between the light source and the point on the focal line.

Note that, the model that has been explained here, describes the propagation pattern that is caused by the effect of a single cell. This model is utilized as the building block to simulate a more complicated channel model including numerous cells of different types in multiple layers to obtain a more realistic model of the light propagation in a human blood vessel by considering the movements of the cells.

3.2 Random Positioning and Movements of the Cells

The heart is the driver of the circulatory system by pumping blood through rhythmic contraction and relaxation. The rate of blood flow out of the heart (often expressed in L/min) is known as the cardiac output. Blood being pumped out of the heart first enters the aorta, the largest artery of the body. It then proceeds to divide into smaller and smaller arteries, then into arterioles, and eventually capillaries. In a healthy circulatory system, the volume of blood returning to the heart each minute is approximately equal to the volume that is pumped out each minute (the cardiac output). Because of this, the velocity of blood flow across each level of the circulatory

system is primarily determined by the total cross-sectional area of that level. This is mathematically expressed by the following equation:

$$v_{blood} = Q/A, \quad (6)$$

where v_{blood} is the velocity of the blood in cm/s, Q is the blood flow in ml/s, and A is the cross sectional area in cm^2 . This value is inversely related to the total cross-sectional area of the blood vessel and also differs per cross-section. The blood flow velocity is the fastest in the middle of the vessel and slowest at the vessel wall. In most cases the mean velocity is used.¹⁸ The fastest speed is in the aorta which around 40 cm/s, and the slowest capillaries which is close to 0.03 cm/s.^{21,22}

The velocity of the blood v_{blood} can be considered as the speed of the RBCs. However, this speed is only useful for the scenario in which the nanomachines are fixed and not moving. In the case that the nanomachines are also moving at the same speed of the RBCs, a much slower relative speed for the cell movements should be considered. As explained earlier in Section 2.2, we consider that the cells are moving following the Brownian motion phenomenon. To simulate the movements of the RBCs in a blood vessel, first we randomly place a number of cells with predefined radii inside a section of a vessel which contains two nanomachines. Then, by following a random motion algorithm, in each step we find the new position of each of the cells through the Weiner process.

3.3 Modulation Technique

We consider a simplex communication between the nanomachines by using a simple Amplitude Shift Keying (ASK) modulation called On-Off Keying (OOK). This communication and modulation scheme is a promising technique to be used for *in vivo* optical communications for several reasons. First of all, due to the processing and power limitations of nanomachines, complicated modulations are not feasible. Secondly, the amount of information and the bandwidth that is needed for communications between the nanomachines is very small, also the environmental optical noise in the human blood vessel is minimum; therefore the nanomachines can communicate through simple small messages that does not require complex coding and modulation schemes. Finally, due to the complicated changes in the polarization of the light as well as the dispersion and scattering phenomena, the detection of the high order modulation and coding schemes are not feasible in such tiny nanomachines with limited processing capabilities.

In OOK, the presence of a carrier for a specific duration represents a binary one, while its absence for the same duration represents a binary zero. Some more sophisticated schemes vary these durations to convey additional information or prevent errors to happen. In our case we consider a raised cosine pulse with the following definition:

$$pulse(t) = \begin{cases} E_0, & |t| \leq \frac{\Delta t}{2} \\ \frac{E_0}{2} \left[1 + \cos \left(\frac{\pi}{\beta \Delta t} \left[|t| - \frac{\Delta t}{2} \right] \right) \right], & -\frac{\Delta t}{2} < |t| \leq \frac{\Delta t}{2}, \\ 0, & \text{otherwise} \end{cases} \quad (7)$$

where E_0 is the electric field intensity at the antenna, Δt is the duration of the pulse, and β is the roll-off factor of the raised cosine pulse. A train of pulses spread in time with redundant bits as the error control technique is considered for the communication between the nanomachines.

4. SIMULATION AND NUMERICAL RESULTS

The electromagnetic wave propagation simulations has been done by using COMSOL Multiphysics. A random motion generator algorithm is utilized to update the location of the cells and the simulations has been done independently for each step since the speed of changes in the channel characteristics considered to be much slower than the duration of the transmitted pulses.

Figure 3 shows the light propagation through a number of randomly positioned RBCs in blood plasma for two different antenna sources, (a) a point dipole antenna, and (b) a port antenna which mimics the propagation of a plane wave. The point dipole antenna is the more realistic case for the short communication distances of

nanomachines with their tiny sizes, and the port antenna models the wave propagation for further distances from the antenna that can be considered as plane wave. As it can be seen in this figure, the light is significantly amplified at some rays along the path and at the photon detector receiver line. Thanks to the focusing capability of the RBCs, the signal detection will be easier with higher SNR in presence of the RBCs in blood, which results in longer distance communications.

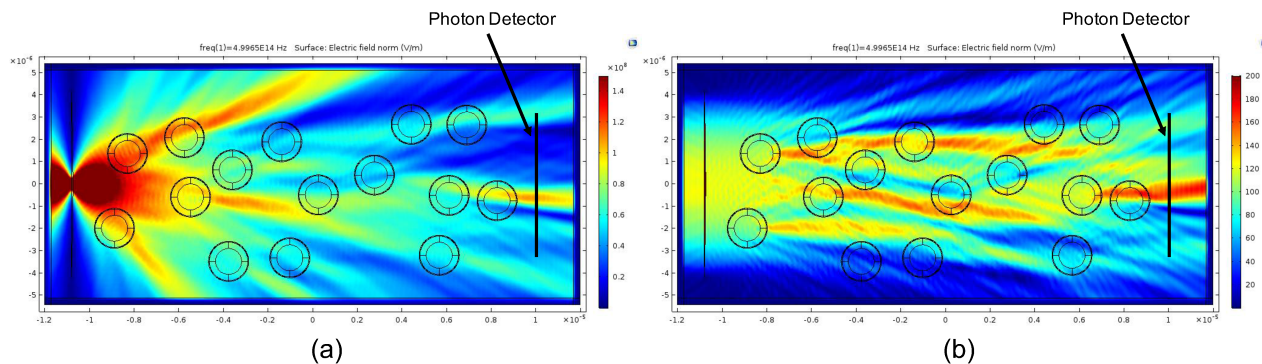


Figure 3. Video 1 shows an animated plot of E-field with moving RBCs inside a human Blood Vessel. The figures above show the screenshots at a given time when light shines from (a) a point dipole antenna; (b) a port antenna. <http://dx.doi.org/10.1117/12.2262824.1>

Figure 4 shows the electric field intensity for 20 independent time steps on a photon detector line (area in 3D) for three different speeds of the cells (a) slow, (b) medium, and (c) fast. We consider the diameter of each of the RBCs to be equal to $7\ \mu\text{m}$, and the cells move $0.2\ \mu\text{m}$, $1.4\ \mu\text{m}$ and $2\ \mu\text{m}$ in each time step for the slow, medium and fast speeds respectively. By considering the fastest speed of the cells which is about $40\ \text{cm/s}$ in aorta, the maximum width of the pulse Δt for which the channel characteristics do not change due to the cell movements is considered to be $0.5\ \mu\text{s}$ which is 10 times shorter than the time steps used for the simulations.

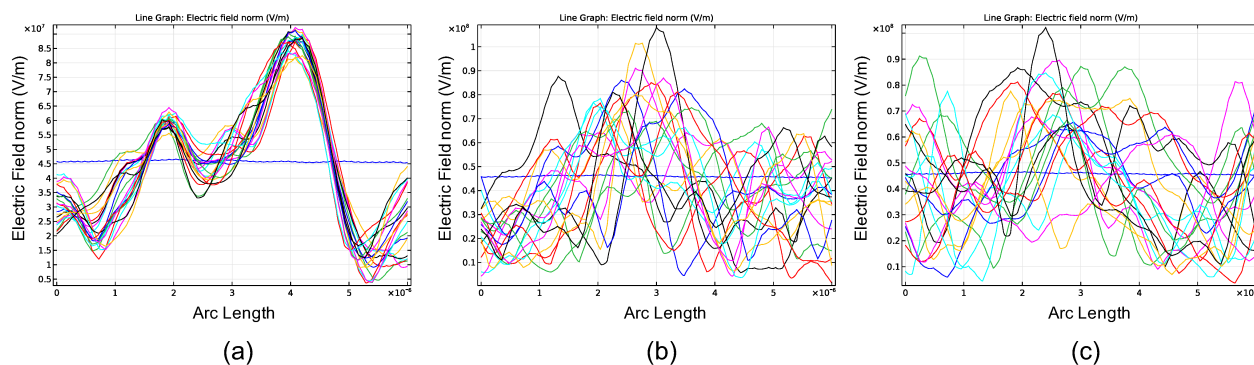


Figure 4. Received E-field at the Detector Line. Cells are moving at a (a) slow; (b) medium; (c) fast speed.

The straight blue line shows the received signal in case of having no cells in between the antenna and the detector. As it can be seen in Figure 4 (a), for the slow motion scenario the amplified field tends to be around a certain area of the detector. This is the scenario in which the nanomachines are moving with the cells at the same speed and the relative motion of the cells and nanomachines is minimal. A maximum photon detector works well for this scenario since the channel is predictable as time goes on. On the other hand, the fast movements of the cells Figure 4 (c), cause the peak of the received signal to be moving faster over different areas of the photon detector. For this scenario, which happens when the nanomachines are fixed (such as implanted nano-devices) and the cells are moving, an integrator photon counter which counts all the received photons all over the area of

the detector is preferred.

Figure 5 shows the path loss in a distance from the antenna for two different detectors (a) integrator photon counter (b) maximum field intensity detector. The results are shown for three different sizes of the detector, namely, $0.36\ \mu\text{m}$, $0.9\ \mu\text{m}$ and $1.8\ \mu\text{m}$ for the length of the receiver antenna. As it can be seen in Figure 5 (a) for the integrator detector, the bigger the area of the antenna the lower the path loss. However, for the peak detector the size of the receiver antenna does not play a significant role until long distances in which the chance of detecting the focused field is higher if we use bigger antennas. It is worth noting that since we are showing the path loss only for one random position of the cells in these figures, there are some fluctuations in the path loss due to the focusing property of the cells along the path. However, by averaging over a large enough number of simulations with random positions, these curve will become smoother. Furthermore, Figure 5 shows that the path loss decrease 10 dB in average when we have the RBCs in between the communicating nanomachines. This interesting phenomenon happens due the focusing capability of the RBCs that act as micro-fluidic optical lenses.

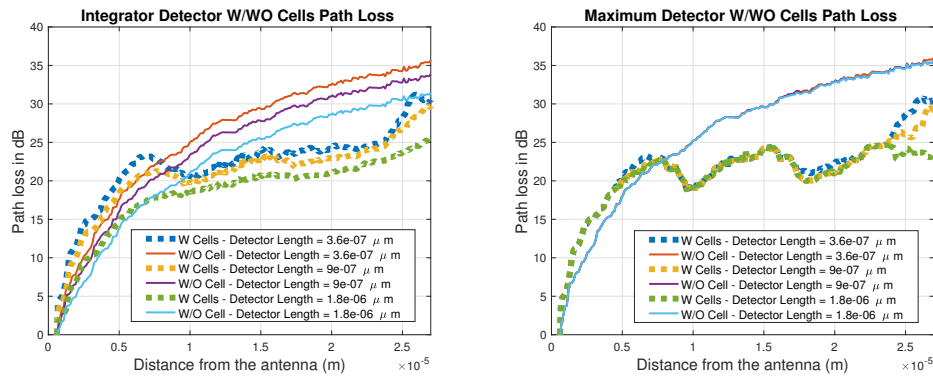


Figure 5. Path loss in dB versus distance from the antenna with (a) integrator detector; (b) maximum detector.

5. CONCLUSIONS

In this paper, we have developed an optofluidic channel model and studied the communication properties and temporal dynamics between a pair of *in vivo* nanomachines in the human blood vessel. The developed model has been built upon light propagation modeling through multi-layered single cells and cell assemblies and we have taken into account the geometric, electromagnetic and microfluidic properties of red blood cells in the human circulatory system.

We have shown that the speed of the cell movements and the size of the antenna are the key factors for *in vivo* optical communications. Two different scenarios has been taken into account, in which the nanomachines are either floating with the cells inside the vessel or are fixed as implants closed the blood vessel wall. For slow movements of the cells a peak detector with a rather small antenna works well for short range communications. However, for larger distances or fast movements of the cells, an integrator photon counter performs better in terms of path loss. The results also shows that an average of 10 dB gain is obtained when there are multiple cells in between the communicating nanomachines.

The proposed model will not only guide the development of practical communication strategies among nanosensors, but also enables new nano-biosensing strategies able to identify diseases by detecting the slight changes in the channel impulse response, caused by either the change in shape of the blood cells or the presence of pathogens. Compared to *ex vivo* measurements, which are conducted on samples extracted from the human body, iWNSNs promise to engender significant contributions to our understanding of (sub) cellular processes under normal and diseased conditions when and where they occur.

ACKNOWLEDGMENTS

This work was supported by the U.S. National Science Foundation (NSF) under Grants No. CBET-1445934 and No. CBET-1555720.

REFERENCES

- [1] Renault, R., Sukenik, N., Descroix, S., Malaquin, L., Viovy, J.-L., Peyrin, J.-M., Bottani, S., Monceau, P., Moses, E., and Vignes, M., "Combining microfluidics, optogenetics and calcium imaging to study neuronal communication in vitro," *PloS one* **10**(4), e0120680 (2015).
- [2] Schmid, F., Wachsmuth, L., Schwalm, M., Prouvot, P.-H., Jubal, E. R., Fois, C., Pramanik, G., Zimmer, C., Faber, C., and Stroh, A., "Assessing sensory versus optogenetic network activation by combining (o) fmri with optical ca2+ recordings," *Journal of Cerebral Blood Flow & Metabolism* , 0271678X15619428 (2015).
- [3] Khajavikhan, M., Simic, A., Katz, M., Lee, J., Slutsky, B., Mizrahi, A., Lomakin, V., and Fainman, Y., "Thresholdless nanoscale coaxial lasers," *Nature* **482**(7384), 204–207 (2012).
- [4] Nafari, M. and Jornet, J. M., "Modeling and performance analysis of metallic plasmonic nano-antennas for wireless optical communication in nanonetworks," *IEEE Access* (2017).
- [5] Tang, L., Kocabas, S. E., Latif, S., Okyay, A. K., Ly-Gagnon, D.-S., Saraswat, K. C., and Miller, D. A., "Nanometre-scale germanium photodetector enhanced by a near-infrared dipole antenna," *Nature Photonics* **2**(4), 226–229 (2008).
- [6] Wirdatmadja, S. A., Balasubramaniam, S., Koucheryavy, Y., and Jornet, J. M., "Wireless optogenetic neural dust for deep brain stimulation," *IEEE 18th International Conference on e-Health Networking, Applications and Services (Healthcom)* , 1–6 (2016).
- [7] Akyildiz, I. F., Brunetti, F., and Blázquez, C., "Nanonetworks: A new communication paradigm," *Computer Networks* **52**(12), 2260–2279 (2008).
- [8] Akyildiz, I. F., Pierobon, M., Balasubramaniam, S., and Koucheryavy, Y., "The internet of bio-nano things," *IEEE Communications Magazine* **53**(3), 32–40 (2015).
- [9] Pierobon, M. and Akyildiz, I. F., "Capacity of a diffusion-based molecular communication system with channel memory and molecular noise," *IEEE Transactions on Information Theory* **59**(2), 942–954 (2013).
- [10] Jornet, J. M. and Akyildiz, I. F., "Graphene-based plasmonic nano-antenna for terahertz band communication in nanonetworks," *IEEE Journal on selected areas in communications* **31**(12), 685–694 (2013).
- [11] Pope, R. M. and Fry, E. S., "Absorption spectrum (380–700 nm) of pure water. ii. integrating cavity measurements," *Applied optics* **36**(33), 8710–8723 (1997).
- [12] Jacques, S. L., "Optical properties of biological tissues: a review," *Physics in medicine and biology* **58**(11), R37 (2013).
- [13] Wang, L. V. and Wu, H.-i., [*Biomedical optics: principles and imaging*], John Wiley & Sons (2012).
- [14] Lin, J. C., [*Electromagnetic fields in biological systems*], CRC press (2011).
- [15] Guo, H., Johari, P., Jornet, J. M., and Sun, Z., "Intra-body optical channel modeling for in vivo wireless nanosensor networks," *IEEE transactions on nanobioscience* **15**(1), 41–52 (2016).
- [16] Johari, P. and Jornet, J. M., "Nanoscale optical channel modeling for in vivo wireless nanosensor networks: A geometrical approach," *Proc. of the IEEE International Conference on Communications*, (2017).
- [17] Miccio, L., Memmolo, P., Merola, F., Netti, P., and Ferraro, P., "Red blood cell as an adaptive optofluidic microlens," *Nature communications* **6** (2015).
- [18] Tortora, G. J. and Derrickson, B., "The cardiovascular system: blood vessels and hemodynamics," *Principles of anatomy and physiology* , 610–635 (2012).
- [19] Thiriet, M., [*Biology and mechanics of blood flows: Part II: Mechanics and medical aspects*], Springer Science & Business Media (2007).
- [20] Rand, P. W., Lacombe, E., Hunt, H. E., and Austin, W. H., "Viscosity of normal human blood under normothermic and hypothermic conditions," *Journal of Applied Physiology* **19**(1), 117–122 (1964).
- [21] Thurston, G. B., "The viscosity and viscoelasticity of blood in small diameter tubes," *Microvascular research* **11**(2), 133–146 (1976).
- [22] Marieb, E. and Hoehn, K., "The cardiovascular system: blood vessels," *Human anatomy & physiology* , 703–720 (2004).